JOURNAL OF MATERIALS SCIENCE 8 (1973) 1567–1572

Thermally activated flow parameters in the deformation of MgO single crystals

M. SRINIVASAN, T. G. STOEBE
Division of Metallurgical Engineering, University of Washington, Seattle, Washington, USA

Strain-rate cycling methods have been used to determine the thermally activated flow parameters in the compressive deformation of MgO single crystals. Activation volumes of the order of $100\mathbf{b}^3$ have been measured for deformation below room temperature, indicating dislocation-point defect interactions as the rate controlling mechanism for hardening at these temperatures, while V^* values of the order of $1000\mathbf{b}^3$ have been measured at and above room temperature. This, together with the fact that the effective stress remains constant with strain at these temperatures identifies the interaction of dislocations with dislocation dipoles as the rate controlling mechanism in this temperature range. The Gibbs free energy for deformation, ΔG, equals the activation enthalpy, ΔH, at low temperatures and the deviation of ΔG from ΔH above room temperature may be attributed to entropy effects.

1. Introduction

Thermally activated flow in a crystalline material is a dynamic process and has been studied quite extensively in bcc and fcc metals and alloys. However, the use of the thermally activated flow parameters in identifying the deformation mechanisms in the case of ionic solids has not yet been widely used. In MgO, for example, the relative contributions of the thermal and athermal stresses to the work hardening have not been established, nor has the activation volume and the activation enthalpy behaviour as a function of stress, strain, and temperature. In this paper, the thermally activated flow parameters obtained in the deformation of MgO single crystals will be critically analyzed for the magnitude of the activation parameters and their temperature, stress, and strain dependence, to assist in identifying the rate controlling mechanism for deformation in this material.

2. Experimental procedures and analysis

Single crystals of MgO were obtained from the Oak Ridge National Laboratories. A spectrographic analysis of these crystals showed the following impurity composition: Fe, 0.005%; Si, 0.007%; Mn, 0.001%; Al, 0.007%; Cu, 0.0005% and Ca, 0.005%, where the analysis is reported as oxides of the elements indicated. These crystals were deformed from 77 to 673 K using a jig attached to the Instron machine [1].

The thermal activation parameters were obtained primarily from strain-rate cycling experiments. On the assumption that the dislocation density and internal stress (τ_μ) remain constant during strain change, the effective stress τ^* can be evaluated from the experimental data using the relation [2],

$$\tau^* = \frac{m^*}{m'} \cdot \tau_a, \tag{1}$$

where τ_a is the applied stress,

$$m' = \frac{\Delta \ln \dot{\epsilon}}{\Delta \ln \tau}, \tag{2}$$

and m^* is the value obtained by extrapolating m' to zero strain. Strain-rate change ratios, $\dot{\epsilon}_2/\dot{\epsilon}_1$, of 40, 20, 10 and 4 were used in these experiments, with a base strain-rate of 5×10^{-4} min^{-1}. Once τ^* is thus known, the internal stress τ_μ is obtained from the relation,

$$\tau_\mu = \tau_a - \tau^*. \tag{3}$$

The double strain-rate change experiment was also used at room temperature with three strain-rates in such a way that $\dot{\epsilon}_1/\dot{\epsilon}_2 = \dot{\epsilon}_2/\dot{\epsilon}_3$. Assuming that the dislocation density remains constant during the strain-rate change, the

internal stress can be calculated using the equation [2]

$$\tau_\mu = \frac{\tau_2 - \tau_1\tau_3}{2\tau_2^2 - (\tau_1 + \tau_3)} \cdot \quad (4)$$

From this, a plot of τ_a, τ^*, and τ_μ versus strain will indicate the relative contributions of the internal stress and the effective stress in plastic flow.

The experimental activation volume, V^*, may be calculated from the relation,

$$V^* = kT\left(\frac{\triangle \ln\dot{\epsilon}}{\triangle\tau}\right)_T, \quad (5)$$

where k is the Boltzmann's constant, T is the absolute temperature, and $\triangle\tau$ is the change in shear stress resulting from a change in strain-rate. A plot of V^* versus τ^* can then be constructed, using τ^* from Equation 1.

The activation enthalpy, $\triangle H$, was calculated from the strain-rate cycling data and the temperature dependence of flow stress data [1] using the relation [3]

$$\triangle H = -kT^2\left(\frac{\triangle \ln\dot{\epsilon}}{\triangle\tau}\right)_T\left(\frac{\triangle\tau}{\triangle T}\right)_{\dot{\epsilon}} \quad (6)$$

If it is assumed that the entropy varies only slowly with stress (temperature), Evans and Rawlings [3] arrive at the expression,

$$\triangle H = \triangle H_0 - \int_0^{\tau^*} V^* \, d\tau^* \cdot \quad (7)$$

Here $\triangle H_0$ is the total activation enthalpy at zero effective stress. Thus numerical integration of the V^* versus τ^* plot can be used to determine $\triangle H_0$ as a function of effective stress.

The experimental data obtained can be used to evaluate the Gibbs activation free energy, since Gibbs [4] and Schoeck [5] have shown that

$$\triangle G = \frac{\triangle H + T(d\mu/dT)(\tau^*/\mu)V^*}{1 - (T/\mu)(d\mu/dT)} \cdot \quad (8)$$

The shear modulus, μ, has been calculated as $\mu = [C_{44}(C_{11} - C_{12})/2]^{\frac{1}{2}}$, where the C_{ij} values for MgO are obtained from a published compilation [6] and $d\mu/dT$ can be obtained from the temperature dependence of the shear modulus data.

3. Experimental results

3.1. Strain dependence of thermal and athermal stresses

The effective stress at various temperatures as a function of strain has been determined in this work primarily by strain-rate change methods using Equation 1. In these experiments it has been observed [1] that during the early stages of deformation (low strains) at most temperatures, the applied stress is almost entirely owing to the effective stress τ^*. As deformation proceeds, the effective stress remains practically constant with strain, while the internal stresses increase in almost an identical manner to the applied stress, contributing to work-hardening. As the temperature approaches T_0, the temperature at which the effective stress drops to zero, τ^* decreases and $\tau\mu$ increases. The critical temperature T_0 for these crystals is about 700 K.

The determination of τ^* and τ_μ has also been performed using the double strain-rate change method, the stress relaxation method, and the dip test (incremental unloading technique [7]). In these experiments the applied stress is indicated [8] to be almost entirely owing to the internal stress τ_μ. The results of the double strain-rate change tests conducted at room temperature for MgO crystals is shown in Fig. 1. Here again, strain dependence of the applied stress is similar to that of the internal stress.

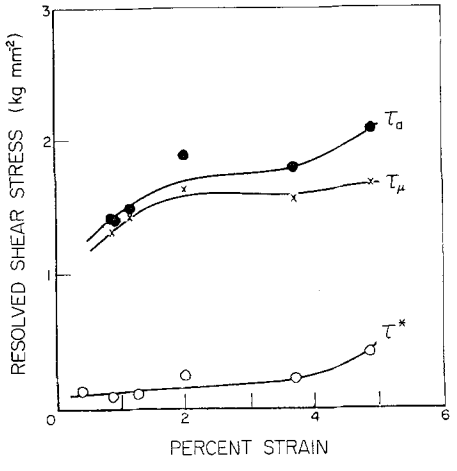

Figure 1 Separation of athermal and thermal stresses from applied stress at room temperature by the double strain-rate cycling method.

3.2. Effective stress dependence of the strain-rate sensitivity

The change in shear stress ($\triangle\tau$) during a change in strain-rate for one strain-rate change ratio (40), as a function of effective stress, for temperatures 77 to 673 K is shown in Fig. 2. There is

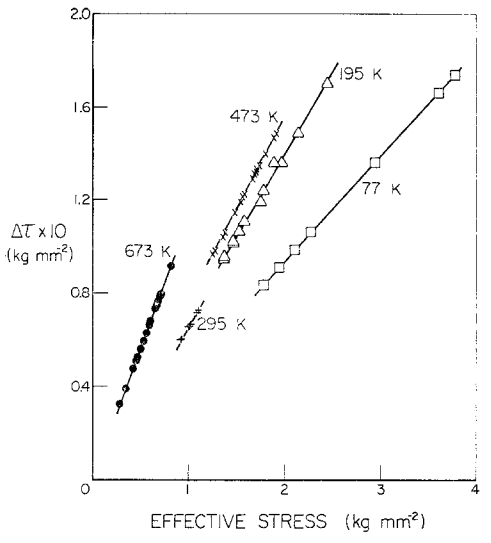

Figure 2 The effective stress dependence of the strain-rate sensitivity for deformation temperatures indicated in MgO single crystals. Strain-rate change ratio used is 40.

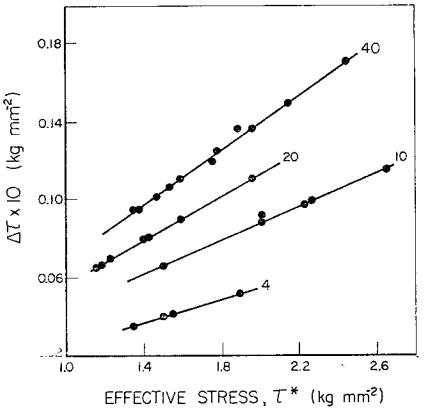

Figure 3 Strain-rate change ratio dependence of strain-rate sensitivity at 195K. Strain-rate ratios are indicated.

a very strong dependence of strain-rate sensitivity on the effective stress. The strain-rate sensitivity of the flow stress also depends strongly on the strain-rate change ratio used in the strain-rate change; for example at $\tau^* = 2$ kg mm^{-2}, for 195K, changing the strain-rate ratio from 40 to 4 reduces the observed $\triangle\tau$ by three times. The effect of strain-rate change ratio in a strain-rate cycling experiment on the change in shear stress ($\triangle\tau$) is shown in Fig. 3, which was obtained for deformation at 195K.

The temperature dependence of $\triangle\tau$, extrapolated to yielding, for the strain-rate change ratio of 40 is shown in Fig. 4. The strain-rate sensitivity of the flow stress approaches zero at the deformation temperature of 673K, in agreement with the temperature dependence of the effective stress [1].

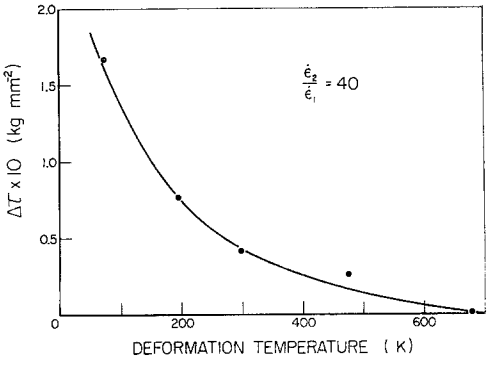

Figure 4 Temperature dependence of the strain-rate sensitivity; data shown is for strain-rate change ratio of 40.

TABLE I Temperature and strain dependence of the average activation volume

	V^*/b^3					
	Deformation temperature (K)					
% strain	77	125[b]	195	295	473[a]	673[a]
0.5	100	109	310	790	1000	3500
1.0	118	164	336	812	948	3200
2.0	142	216	346	947	860	2550
3.0	179	211	343	864	800	2375
4.0	182	227	—	—	760	2100
5.0	200	230	—	—	725	1900

[a]For one strain-rate cycling test for $\dot{\epsilon}_2/\dot{\epsilon}_1 = 40$ only.
[b]For one strain-rate cycling test for $\dot{\epsilon}_2/\dot{\epsilon}_1 = 20$ only.

3.3. Activation volume

In this work, the activation volume has been obtained from strain-rate cycling experiments using Equation 5. Table I gives the average activation volume obtained for different strain-rate ratios in the strain rate cycling experiments, as a function of strain and deformation temperature. At and below room temperature, V^* is seen to increase slightly with strain while above room temperature, V^* decreases with strain. Fig 5a and b show the activation volume as a function of effective stress at temperatures from 77 to 673K. As the temperature increases, the effective stress decreases and the activation volume

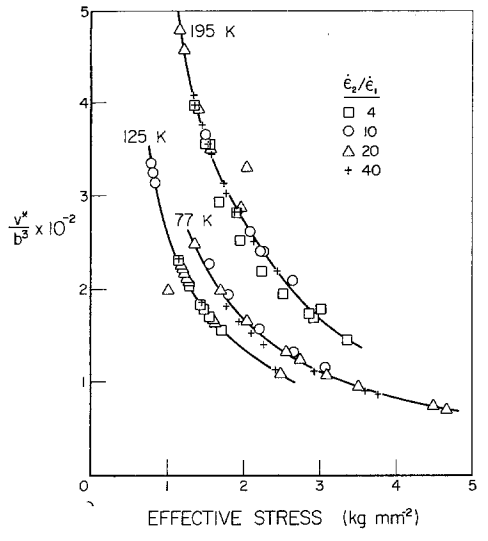

(a)

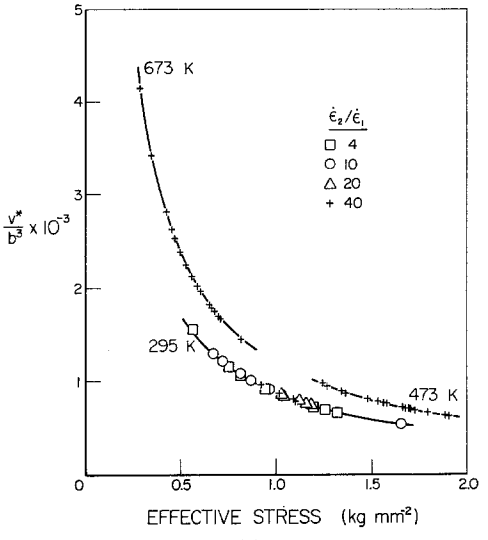

(b)

Figure 5 Effective stress dependence of activation volume, (a) for deformation temperatures below room temperature, (b) for deformation temperatures at and above room temperature.

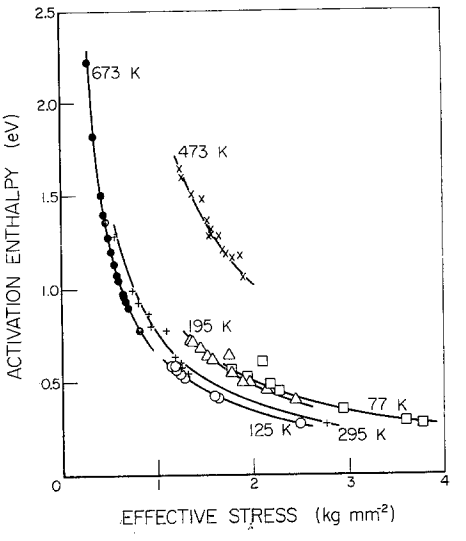

Figure 6 Effective stress dependence of activation enthalpy at deformation temperatures indicated.

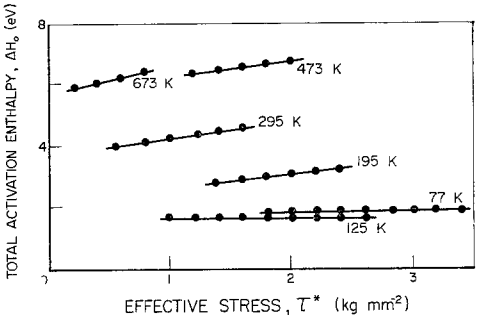

Figure 7 Temperature and effective stress dependence of total activation enthalpy.

increases, with the same dependence being noted for all strain-rate ratios used at a given temperature.

3.4. Activation energies

The activation enthalpy has been calculated at each temperature using Equation 6 and is plotted as a function of effective stress in Fig. 6 for deformation temperatures from 77 to 673 K. The activation enthalpy is seen to decrease with increasing effective stress. The total activation enthalpy for deformation, $\triangle H_0$, obtained using Equation 7, is plotted as a function of effective stress in Fig. 7. Here, $\triangle H_0$ is seen to be fairly constant below room temperature, increasing slightly above room temperature with increasing effective stress. The activation free energy, calculated using Equation 8, is shown in Fig. 8a; and entropy values, obtained as $\triangle S = (\triangle H - \triangle G)/T$ are shown in Fig. 8b. These entropy values are seen to be markedly influenced by the deformation temperature.

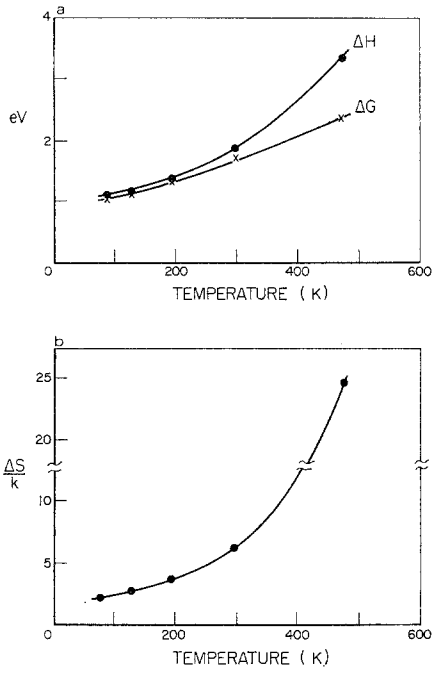

Figure 8 (a) The temperature dependence of activation energy and enthalpy in MgO deformation. (b) The entropy contribution to plastic flow as a function of deformation temperature, in MgO single crystals.

4. Discussion

4.1. Strain-rate sensitivity of the flow stress

The determination of strain-rate sensitivity as a function of effective stress has been found to be useful in the mechanical behaviour of b c c materials and has been widely used, for example, by Spitzig and Keh [9] for iron single crystals. If a lattice friction stress is responsible for the flow characteristics, $\triangle\tau$ should be independent of effective stress. However, it has been shown that this requirement should be coupled with the requirement that the mobile dislocation density also be independent of effective stress [10]. Unfortunately, the behaviour of the mobile dislocation density as a function of effective stress is not known in the present case. The results, however, do show a strong dependence of $\triangle\tau$ on effective stress at all temperatures, probably indicating that the lattice friction mechanism may, in fact, be ruled out as operating in the deformation of MgO single crystals at these temperatures.

The temperature variation of $\triangle\tau$ (Fig. 4) agrees with the predictions of the rate analysis of thermally activated flow. At 673K, it becomes zero and deformation at temperatures greater than 673K gives rise to negative strain-rate sensitivity owing to the onset of dynamic strain ageing [11].

4.2. Activation volume

The determination of the activation volume and its temperature, stress and strain dependence assists in identifying the rate-controlling deformation mechanism. The Peierls-Nabarro type activation mechanism requires V^* to be low, of the order of $20\mathbf{b}^3$. The much higher activation volume values obtained here confirm the absence of this mechanism as the rate-controlling factor. A possible mechanism consistent with the V^* values obtained below room temperature seems to be point defect-dislocation interactions [3]. This also fits in well with the observed temperature dependence of the work-hardening behaviour in these crystals [1].

Above room temperature, the activation volume behaviour seems to identify the interaction of dislocations with dislocation dipoles as the rate-controlling process, since V^* decreases as the dipole density increases with strain. An alternate explanation invoking the dislocation intersection mechanism would also show V^* decreasing with strain as the "forest" dislocation density increases. However, τ^* should increase with strain in the dislocation intersection mechanism [3]. Experimentally, τ^* remains constant with strain above room temperature. Hence the dislocation intersection mechanism can be ruled out and the interaction of dislocations with dislocation dipoles may be identified as the activation mechanism for the compression of MgO single crystals above room temperature.

The activation volume obtained at 473K, $1000\mathbf{b}^3$ is comparable to the value of $1310\mathbf{b}^3$ obtained at 446K by Moon and Pratt [12] for MgO crystals containing about 10 ppm Fe^{+3}. Kumar [13] has found an activation volume of $25\mathbf{b}^3$ at low temperatures, increasing to $56\mathbf{b}^3$ on rapid quenching from 1000°C, and rules out the Peierls mechanism in favour of impurity controlled mechanisms. In the present study, the activation volume is greater since the Fe^{+2} impurity in the present case is not as strong a hardener in MgO as the Fe^{+3} impurities which would have been effective in Kumar's work. The activation volume data obtained for different strain-rate ratios in a strain rate cycling experiment falls on the same curve, as noted in Fig. 5.

4.3. Activation energies

The activation enthalpy behaviour with respect to the effective stress follows a pattern well known in the deformation of other materials. As the temperature increases, the effective stress decreases, and the energy for thermally activated dislocation motion increases. According to Evans and Rawlings [3], if the total activation enthalpy $\triangle H_0$ is independent of stress, it is indicative that a single process is rate controlling. This seems to be so in the present case, at least below room temperature. The slight increase in $\triangle H_0$ with stress at and above room temperature may be owing to entropy effects. The entropy behaviour with respect to temperature shows that entropy depends strongly on temperature. This result is similar to that obtained by Cagnon [14] in LiF, and the entropy values are comparable to his data. The sources of entropy have been discussed by Cagnon [14], the main source being the variation of the shear modulus with temperature arising from a change in the atomic vibrational spectrum with temperature. It should be noted that the experimental determination of thermally activated flow parameters yield only the enthalpy change during the activation event, while theoretical models deal with the corresponding Gibbs free energy. Hence, as pointed out by Schoeck, [5] the entropy term should not be discarded when analysing experimental data.

Further, the incorporation of a hyperbolic sine term into the dislocation velocity equation, as suggested by Li [15], and the possible influence of back fluctuations at high temperatures [16], can also lead to a slight increase in $\triangle H_0$ with effective stress. In the light of these observations and the present data, it may be concluded that a singly thermally activated mechanism is operative in MgO single crystals over the range of the present measurements.

5. Summary and conclusions

The determination of activation parameters has been useful in identifying the rate controlling mechanism in the thermally activated deformation of MgO single crystals. The activation volume data obtained at 77 to 295 K are useful here, since they confirm that a dislocation-point defect interaction mechanism is rate controlling. Above room temperature, the activation volume data indicates that the dislocation dipole intersection mechanism may be rate controlling.

The presence of singly thermally activated deformation mechanisms are indicated for the temperatures between 77 and 673 K. Below room temperature, the total activation enthalpy is constant with effective stress, again indicating that a single mechanism is operating. However, at and above room temperature, entropy effects cannot be neglected in the activation analysis.

Acknowledgements

Our thanks are extended to Dr Charles Butler of the Oak Ridge National Laboratory for supplying the MgO crystals and to Dr Lambert Bates of the Battelle Northwest Laboratories for assistance with the high temperature anneal. Financial support for this work from the NASA Ceramic Materials Research Program at the University of Washington is gratefully acknowledged.

References

1. M. SRINIVASAN and T. G. STOEBE, *J. Mater. Sci.* to be published.
2. J. C. M. LI, Canad. J. Phys. **45**, (1967) 493
3. A. G. EVANS and R. D. RAWLINGS, *Phys. Stat. Sol.* **34** (1969) 9.
4. G. B. GIBBS, *Phil. Mag.* **161** (1967) 97.
5. G. SCHOECK, *Phys. Stat. Sol.* **8** (1965) 499.
6. Southern Methodist University, *J. Grad. Research Center*, Dallas Texas (1965) pp. 192-8.
7. C. N. AHLQUIST and W. D. NIX, *Scripta Met.* **3** (1969) 679.
8. M. SRINIVASAN, Ph.D. Thesis, University of Washington (1972).
9. W. A. SPITZIG and A. S. KEH, *Acta Metallurgica* **18** (1970) 1021.
10. D. J. BAILEY and W. F. FLANAGAN, *Phil. Mag.* **19** (1963) 1093.
11. M. SRINIVASAN and T. G. STOEBE, *J. Mater. Sci. & Eng.* **12** (1973) 87.
12. R. L. MOON and P. L. PRATT, *Proc. Brit. Ceram. Soc.* **15** (1970) 203.
13. A. KUMAR, *Acta Metallurgica* **16** (1968) 333.
14. M. CAGNON, *Phil. Mag.* **24** (1971) 1465.
15. J. C. M. LI, *Trans. Met. Soc. AMIE* **233** (1965) 219.
16. J. J. JONAS, *Acta Metallurgica* **17** (1969) 397.

Received 30 March and accepted 15 June 1973.